Materials Horizons

COMMUNICATION

View Article Online
View Journal

Cite this: DOI: 10.1039/c8mh01013g

Received 22nd August 2018,
Accepted 18th December 2018

DOI: 10.1039/c8mh01013g

rsc.li/materials-horizons

Controlling the structure and magnetic properties of cluster-assembled metallic glasses†

Cahit Benel,[a] Arne Fischer,[a] Anna Zimina,[bc] Ralph Steininger,[d] Robert Kruk,[a] Horst Hahn*[aef] and Aline Léon ‡*[d]

The potential to control the structure of amorphous materials and establish correlations with their properties would constitute an extraordinary step in formulating new pathways to design and tailor amorphous structures, which correspondingly would exhibit novel properties. Towards achieving this goal, a bottom-up approach is proposed here. In the present study, cluster-assembled $Fe_{80}Sc_{20}$ metallic glasses are used as the model systems to illustrate this potentially groundbreaking approach. Accordingly, $Fe_{80}Sc_{20}$ amorphous films are nanofabricated under well-defined conditions with precise control over cluster size and impact energy. Their local atomic structures are characterized by X-ray absorption spectroscopy around both constituent metals, *i.e.*, Fe and Sc. The capability of controlling the local structure by controlling the deposition energy (*i.e.*, the clusters' impact energy) has resulted in substantial changes in the magnetic Curie temperature. In fact, the Curie temperature changes by as much as 60 K when the deposition energy is increased from 50 eV per cluster (the lowest deposition energy) to 500 eV per cluster (the highest deposition energy). This remarkable result, clearly establishing a structure–property relationship, observed for the first time in cluster-assembled metallic glasses, opens up new pathways for synthesizing novel amorphous materials with engineered structures and accompanying new properties.

Conceptual insights

In this manuscript, we demonstrate an effective method to synthesise cluster-assembled metallic glasses with full control over their atomic structure and magnetic properties. Growth of metallic glass films is performed by means of a novel experimental technique using the energetic impact of size-selected clusters on substrates. Experimental evidence for the correlation between the atomic structures of the constituent atoms (Fe and Sc herein), determined by XANES and EXAFS studies, and the magnetic properties in amorphous materials of $Fe_{80}Sc_{20}$ is provided. Our work demonstrates that the amorphous structure can be drastically different from the known structure of rapidly quenched metallic glasses and, furthermore, can be controlled by the impact energy of the clusters during assembly. In addition, a selected magnetic property, the Curie temperature, is shown to scale with the different local structures, potentially opening new ways to control the properties of the metallic glasses. Therefore, novel amorphous structures exist with distinct structural differences and they are stable over a certain temperature range. The discovery of the different local structures of metallic glasses, combined with the possibility of controlling the structures and magnetic (and potentially other physical) properties in binary metallic glasses, opens new horizons for the design of tailormade amorphous structures.

1. Introduction

Since their original discovery, in 1960 by Duwez's group,[1] metallic glasses have been studied for decades around the world by various research groups. This prolonged interest in this class of materials is partly based on some intriguing fundamental questions regarding the details of the atomic arrangements within the amorphous state and how these arrangements affect their macroscopic properties.[2–8] However, solid and convincing experimental evidence for such a correlation between the structure and properties in the amorphous state is still largely lacking and, consequently, this research topic has been and still is a long-standing challenge to materials

[a] Institute of Nanotechnology, Karlsruhe Institute of Technology, Hermann-von-Helmholtz-Platz 1, 76344 Eggenstein-Leopoldshafen, Germany
[b] Institute of Catalysis Research and Technology, Karlsruhe Institute of Technology, Hermann-von-Helmholtz-Platz 1, 76344 Eggenstein-Leopoldshafen, Germany
[c] Institute for Chemical Technology and Polymer Chemistry, Karlsruhe Institute of Technology, Engesserstr. 18/20, 76128 Karlsruhe, Germany
[d] Institute for Photon Science and Synchrotron Radiation, Karlsruhe Institute of Technology, Hermann-von-Helmholtz-Platz 1, 76344 Eggenstein-Leopoldshafen, Germany. E-mail: aline.leon@Kit.edu
[e] Joint Research Laboratory Nanomaterials at Technische Universität Darmstadt, 64287 Darmstadt, Germany
[f] Herbert Gleiter Institute of Nanoscience, Nanjing University of Science and Technology, Nanjing, China

† Electronic supplementary information (ESI) available. See DOI: 10.1039/c8mh01013g

‡ Current address: European Institute for Energy Research, Emmy Noether Straße 11, 76131 Karlsruhe, Germany. E-mail: aline.leon@eifer.org

scientists. In the present study, we propose a novel synthesis route for producing metallic glasses that makes it possible to finely control their atomic structures, substantially beyond what has been possible using previous approaches and available experimental tools. In particular, in this case study, the aim is to control the magnetic properties of the resulting metallic glass films by closely controlling the structure of the clusters at the local level and then potentially develop insightful new structure–property correlations.

Based on theoretical modeling,[9] *ab initio* molecular dynamics simulation,[10] synchrotron high energy X-ray diffraction,[11] and nano-beam electron diffraction,[12] the atomic arrangements within metallic glasses have been described in terms of local motifs (a number of other terms have been used in the respective references, such as local atomic configurations, short-range order, clusters, *etc.*). It has been predicted that the relative population of local motifs can be used to control the properties of metallic glasses.[13] However, experimental evidence for establishing relationships between the local atomic structure and macroscopic properties is missing due to the limitations of the existing synthesis routes, which are largely based on rapid quenching from either the gaseous (*i.e.* thin film deposition methods) or the liquid state (*i.e.*, melt spinning techniques). An alternative method, mechanical deformation techniques (*i.e.*, ball milling) occurring solely in the solid state, also does not provide the exact control of the experimental parameter to tailor the local atomic structure and to control the physical properties. In an attempt to control local motifs, Kartouzian *et al.*[14] deposited particles in the size range of the local motifs (10–16 atoms) by cluster beam deposition. The amorphous nature of $Cu_{50}Zr_{50}$ films with different coverages per area (film thicknesses) was confirmed by synchrotron X-ray diffraction but the influences of the impact energy on the short-range order or any structure–property relationships were not investigated.[14] Our technique of cluster ion deposition builds on the basic concept of synthesizing metallic glass samples utilizing a controlled bottom-up approach, in which small amorphous clusters, in the size range of a few hundred atoms, are assembled into metallic glass film samples. This tight control over cluster size has paved the way for developing a new and unique capability that makes it possible to change the local motifs by means of controlling the cluster deposition energy. It is precisely this unique capability that differentiates our innovative approach from other cluster synthesis and processing techniques that have been previously used.

The binary metallic system $Fe_{100-x}Sc_x$ has been chosen as the model system for the present study, since it fulfils the prerequisites for easy glass formation,[15] requiring both low eutectic points (at x = 9 at% and 80 at%) and different sizes of the constituent atoms (the radius of the Sc atom is 1.65 Å, whereas the radius of the Fe atom is 1.24 Å). Herein, the production of $Fe_{80}Sc_{20}$ clusters was performed using a custom-designed and -built cluster ion beam deposition system.[16] The cluster size, determined by *in situ* time of flight mass spectrometry, shows a log-normal size distribution with an average value of 800 atoms per cluster and a sigma-value of 0.54. In this way, solid amorphous particles, consisting of a few hundred atoms with narrow size distribution, are deposited on a substrate and the impact energy of the particles is varied from 50 to 500 eV per cluster. The local atomic arrangements (local motifs) around the iron and scandium atoms were probed using X-ray absorption spectroscopy on samples deposited at 50, 100, 200 or 500 eV per cluster. As it will be shown, the size of the local motifs of the cluster-assembled metallic glasses systematically varies with variation in the clusters' impact energy. This interesting result points out to the possibility that by varying the impact energy one can control the atomic structure of the resulting amorphous phase. It will be further shown that this possibility, of being able to vary the local structure by means of the deposition energy, results in a drastic change in the Curie temperature of the $Fe_{100-x}Sc_x$ cluster-assembled amorphous films by as much as 60 K when the deposition (impact) energy is increased from 50 eV (the lowest value) to 500 eV (the highest value).

2. Materials and methods

2.1. Sample preparation

Custom-designed cluster ion beam deposition (CIBD), shown in Fig. 1, allows synthesizing various cluster-assembled materials under ultra-high vacuum conditions with outstanding precision and reproducibility in terms of cluster size, cluster amount, impact energy, and sample homogeneity.[16] The cluster source combines magnetron sputtering with inert gas condensation. The $Fe_{80}Sc_{20}$ target is sputtered, using an argon–helium gas mixture, in a continuous flow mode, inside a liquid nitrogen cooled tubular chamber. The sputtered atoms are cooled down, *via* collisions with helium and argon atoms, to form clusters of a certain size distribution that is closely controlled by several source parameters, such as gas pressure, gas composition (He/Ar), aggregation length and sputtering power. The clusters leave the aggregation zone through an adjustable iris in a supersonic expansion, which effectively stops further cluster growth. The resulting FeSc clusters are accelerated by a series of electrostatic lenses and then fed into a

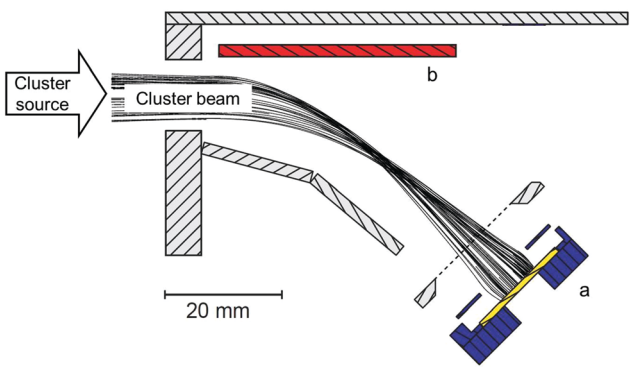

Fig. 1 Cross-sectional view of the deposition stage within the cluster ion beam deposition system that includes simulated ion trajectories, reproduced with the permission of AIP Publishing.[1] The sample holder (a) for the deposition of ionized clusters is shown along with the deflection electrode (b).

continuous channel of electrodes, which guides the clusters to the deposition zone. A series of $Fe_{80}Sc_{20}$ thin films were deposited using the scanning mode with impact energies of 50, 100, 200 or 500 eV per cluster onto silicon substrates, containing native oxide layers at their surfaces. Throughout this paper, the samples are labelled according to their impact energy. The deposition time for each sample was 1 hour, which led to an approximate film thickness of 100 nm (as confirmed through the use of a profilometer). Immediately after the deposition of the $Fe_{80}Sc_{20}$ cluster-assembled films, the samples were protected with a 200 nm thick Mg capping layer, using a thermal evaporator that is directly connected to the deposition chamber. This was done to avoid oxidation of the samples once they became exposed to ambient air for further characterization. One can note that the samples are stable in the temperature range from 5 to 300 K for several weeks. The thermal stability at higher temperature has not been studied so far. For comparison, amorphous ribbons, used as reference, were prepared by melt spinning onto a rotating water-cooled Cu-cylinder. In this paper, these reference samples are labelled RQ or ribbon samples. The energy-dispersive X-ray spectroscopy method was used to confirm and ensure identical chemical compositions for all samples.

2.2. Magnetic measurements

The magnetic properties of the samples were measured using a superconducting quantum interference device (SQUID) magnetometer. The standard zero-field cooled/field cooled (ZFC/FC *vs.* T) curves, between 5 K and 300 K, were measured with an applied field of $\mu_0 H$ = 20 mT, oriented parallel to the sample surface, *i.e.*, along the in-plane direction. In addition, M–H magnetization loops were measured between $\mu_0 H$ = 4.5 T and $\mu_0 H$ = −4.5 T, at 5 K, after having measured field-cooled (FC *vs.* T) curves. The saturation magnetization value was determined from the M *vs.* H loops, by subtracting the linear background, mainly coming from the diamagnetic silicon substrate.

2.3. X-ray absorption spectroscopy

The samples were further analyzed by X-ray absorption fine structure (XAFS) spectroscopy at Fe (7112 eV) and Sc (4492 eV) K-edges. The XAFS spectra were recorded at the SUL-X beamline of the KIT synchrotron facility, using a Si(111) double crystal monochromator. The beam was focused with a Kirkpatrick–Baez mirror system to the sample position to a size of approximately 150 (v) × 250 (h) μm^2. The XAFS spectra were recorded in the fluorescence mode, using a 7 Element Si(Li) fluorescence detector (Gresham, now RaySpec Ltd). The photon energy was calibrated to 7112 eV for the Fe K-edge, using the Fe foil, and to 4465 eV for the Sc K-edge, using the Sn L_1 edge of the Sn foil. Data were processed using the IFEFFIT package[17] in order to account for background correction and normalization.

3. Results and discussion

3.1. Valence states of Sc and Fe

Cluster-assembled samples consisting of reactive elements such as Fe and Sc are prone to oxidation. Therefore, a magnesium capping layer, deposited *in situ*, was used to protect the samples from the ambient air for structure and property characterization. Considering scandium to be the most reactive metal in the FeSc alloy, Sc K-edge X-ray absorption near edge structure (XANES) was recorded on $Fe_{80}Sc_{20}$ cluster-assembled thin films covered with magnesium layers of different thicknesses (10, 50 or 200 nm). The analysis of the spectra indicates that a 200 nm thick Mg layer prevents the oxidation of Sc, while the use of thinner Mg layers results in partial or complete oxidation of the film samples. This trend was further confirmed by the completely different zero field cooled/field cooled (ZFC/FC) magnetization curves, measured on samples with Mg capping layers of 10 nm and 50 nm (see Table S1 and Fig. S1, ESI†), validating the crucial role played by the Mg capping layer in the prevention of oxidation.

3.2. Local structure around Fe and Sc

As the dominant scattered intensity of the protected sample originates mostly from the crystalline Mg-layer, X-ray diffraction could not unfortunately be used to confirm the amorphous structure of the FeSc layer. Similarly, transmission electron microscopy could not be performed as the samples would become completely oxidized during sample preparation and subsequent transfer of the sample to the microscope for TEM analysis. As a consequence, X-ray absorption spectroscopy (XAS) remains the technique of choice to confirm the amorphous structure of the cluster-assembled glasses and also to determine their local motifs (in terms of the number of nearest neighbors and distances to the Fe and Sc scattering centers).

Fig. 2 displays the normalized Sc K-edge XANES spectra (and Fig. S2 – the Fe K-edge XANES, ESI†) of cluster-assembled metallic glasses with 50, 100, and 500 eV impact energy/cluster compared to the spectra of the corresponding metals, Sc_2O_3, and FeSc amorphous ribbon. Analysis of the valence states of Sc and Fe in the cluster-assembled metallic glass samples indicates that Sc and Fe are in the metallic state (as verified by the analysis of the energy positions of the absorption edges; refer to Table S1, ESI†), with an emphasis on the observation that a strong electron correlation effect is present around Sc, which enhances the screening of the Sc nuclear charge in these samples. Comparison to the Sc_2O_3 K-edge position and its fine structure clearly shows that the cluster-assembled samples are not oxidized for all impact energies. Moreover, the shapes of the Sc and Fe K-edge XANES spectra of the cluster-assembled samples are significantly different, when compared either to the corresponding metal foil or to the ribbon, suggesting different local atomic environments in these samples.

The fading of the EXAFS oscillations around Sc and Fe centers in the cluster-assembled metallic glasses, compared to metallic scandium shown in Fig. 3 (and see Fe K-EXAFS data in Fig. S3, ESI†), clearly confirms the amorphous structure of the cluster-assembled samples. The scattering profiles of the three cluster-assembled glass samples at the Sc and Fe K-edges are independent of the impact energy but they exhibit significant differences in shape/amplitude, compared to the corresponding metal, indicating different local structures in the

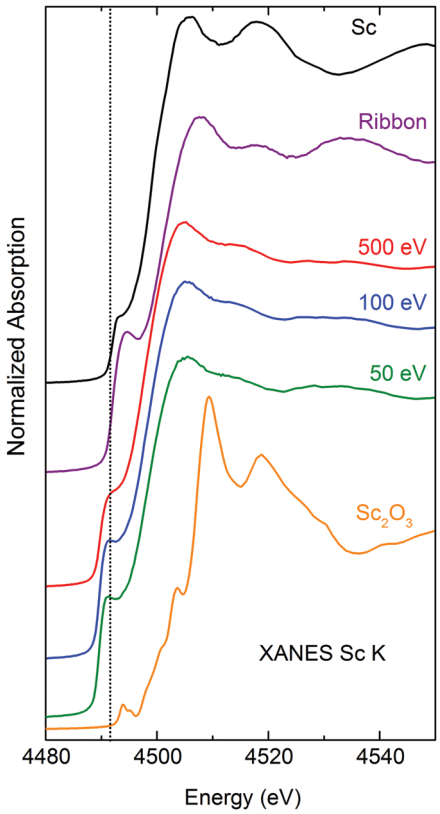

Fig. 2 Normalized XANES region of the Sc K-edge XAS spectra of the RQ ribbon and the cluster-assembled samples deposited with energies of 500, 100, and 50 eV per cluster together with the spectra of Sc and Sc_2O_3. The vertical dashed line at 4492 eV corresponds to the first inflection point in the Sc K-edge XANES spectrum of the pure metal.

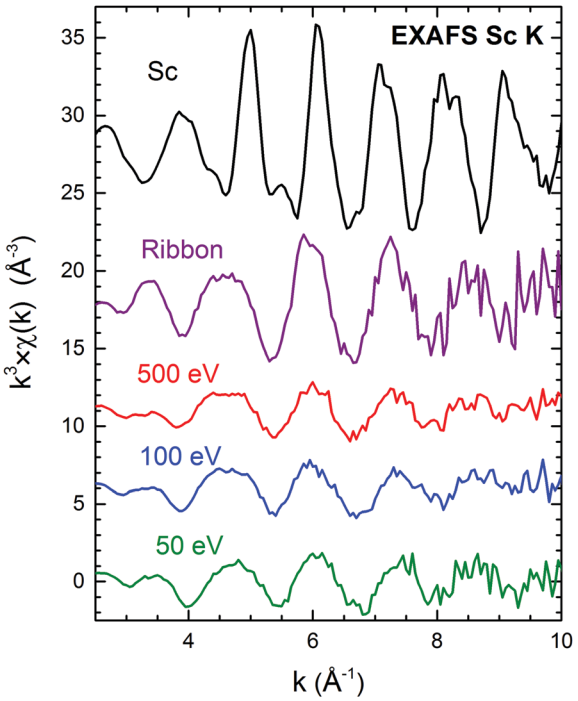

Fig. 3 $k^3 \times \chi(k)$ Sc K EXAFS spectra of the RQ ribbon and cluster assembled metallic glasses deposited with energies of 50, 100 and 500 eV per cluster. The Sc metal is shown for comparison.

cluster-assembled samples. It can be seen that the amplitudes of the oscillations around Sc are significantly lower compared to the amplitudes of the amorphous ribbon or the Sc metal, indicating a sizeable decrease in the number of neighboring atoms around the Sc absorbers. Further information on the local atomic structure around Sc and Fe atoms in the $Fe_{80}Sc_{20}$ cluster-assembled metallic glasses is derived from the detailed analysis of EXAFS spectra. Fig. 4 displays the magnitude of the Fourier transform k^3-weighted EXAFS $\chi(k)$ function of the samples at the Sc and Fe K-edges. A significant reduction of the number of higher order shells, relative to the first order, is observed. This is consistent with the lack of long-range order in the $Fe_{80}Sc_{20}$ cluster-assembled metallic glass samples, irrespective of the impact energy. To quantify the evolution of the structural parameters around Fe and Sc centers, in terms of coordination numbers (N) and interatomic distances (R), with the impact energy, fits of the experimental spectra were performed using single scattering paths generated from theoretical models. The spectrum of the Fe metallic foil can be fitted using the crystallographic data of Fe in the bcc phase ($a = b = c =$ 2.93 Å, space group $Im\bar{3}m$, 8 Fe atoms in the first coordination shell). However, the data of the cluster-assembled samples can only be fitted with a modified Fe structure, assuming an fcc phase ($a = b = c = 3.64$ Å, space group $Fm\bar{3}m$, 12 and 6 Fe atoms in the first and second coordination shells), where 3 Sc replace Fe in the first and second shells (see the fit of the 500 eV impact energy sample, Fig. S4 and S5, ESI†). A summary of the structural parameters around Fe and Sc atoms, obtained from the least-squares fitting, can be found in Fig. 4 (see also Table S2, ESI†). The scattering process involved in these materials was determined by the intensities and shapes of the scattering profiles of Fe and Sc atoms. It should be mentioned that the scattering around the Fe absorber in the cluster-assembled metallic glasses is largely dominated by the scattering of the surrounding iron atoms in the $Fe_{80}Sc_{20}$ structure and less so by the scandium surroundings. By contrast, the scattering at the Sc K edge is sensitive to the presence of the Sc–Fe bond, which can be easily distinguished from the Sc–Sc neighbors. It is evident from the experimental results that the size of the local motifs depends critically on the impact energy of the clusters on the substrate surface. But the Fe–Fe and Fe–Sc distances within the local motifs do not appear to be affected (in fact, these distances remain constant, within the error bar of the experimental data). For the lowest impact energy of 50 eV per cluster, the local motifs consist of only 5 atoms. By contrast, the local motifs of the sample deposited with an impact energy of 500 eV per cluster are substantially larger in size, consisting of 14 atoms per cluster and thus being comparable to those of the rapidly quenched sample.

3.3. Structure–property relationships

In terms of structure–property relationships, we observe that the changes in the internal amorphous structure result in drastic changes in the magnetic properties. In fact, as shown

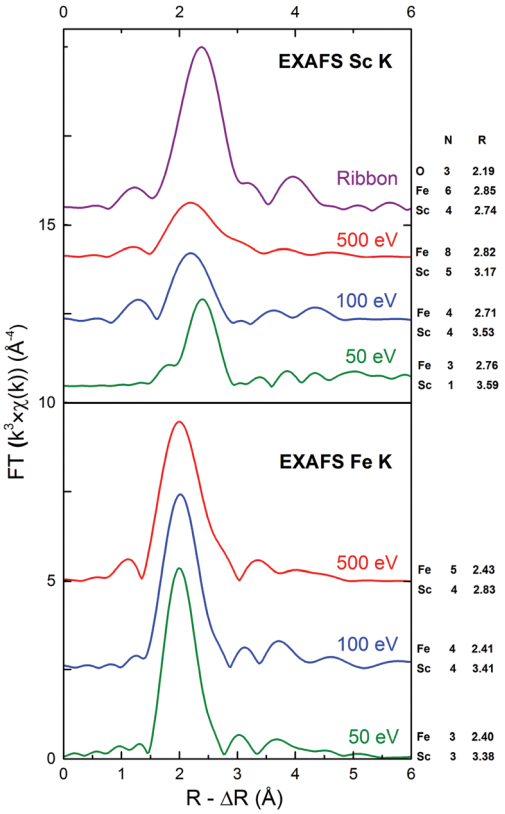

Fig. 4 The magnitudes of the Fourier transform of k^3-weighted EXAFS signals at the Sc and Fe K-edges of the ribbon reference sample and of the cluster-assembled samples deposited with impact energies of 500, 100, and 50 eV per cluster (no phase correction). *N* represents the coordination number and *R* is the interatomic distance in Å for each experimental data resulting from the IFEFFIT fitting procedure (see Table S2 in the ESI†).

in Fig. 5, all samples undergo a paramagnetic to ferromagnetic transition. The magnetic transition temperature (the Curie temperature) shifts from 230 K to 170 K as the impact energy is reduced from 500 eV per cluster to 50 eV per cluster. At low temperatures all samples are ferromagnetic and they display low coercivity as shown by the magnetization loops of the samples measured at 5 K in Fig. S6 (ESI†). As shown in Fig. S7 (ESI†), it can be seen that the measurements are reproducible. This result is consistent with the magnetic phase diagram of amorphous Fe–Sc.[18]

From the structural characterization, it is evident that identical clusters in the cluster beam can lead to different amorphous structures with significantly different magnetic features and Curie temperatures, depending on the impact energy of the clusters. At present, to explain the change in the local motifs as a function of impact energy, it is assumed that the clusters with an average size of 800 atoms per cluster consist of local motifs of similar sizes and compositions to that of the RQ reference sample. The structural modifications, giving rise to the effects seen by EXAFS, may occur in the interfacial regions between the colliding clusters during their assembly into films, with a massive introduction of free volume and changes in the chemical composition during their energetic impact on the substrate.

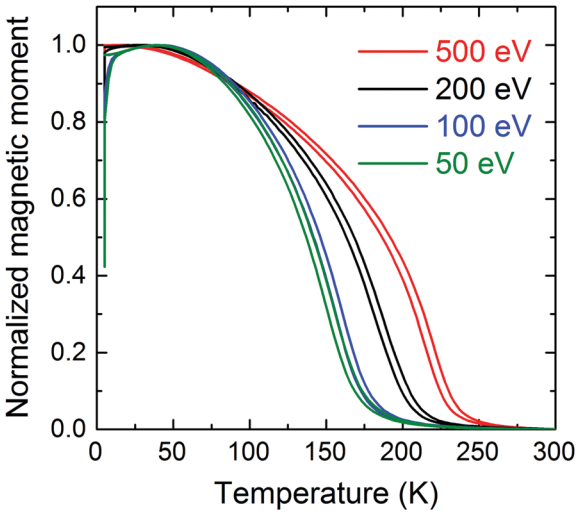

Fig. 5 Temperature dependence of the normalized magnetic moment measured on the $Fe_{80}Sc_{20}$ cluster films deposited on silicon substrates with impact energies of 50, 100, 200, and 500 eV per cluster. The ZFC/FC curves were measured with a SQUID magnetometer and an applied field of $\mu_0 H$ = 20 mT parallel to the sample surface.

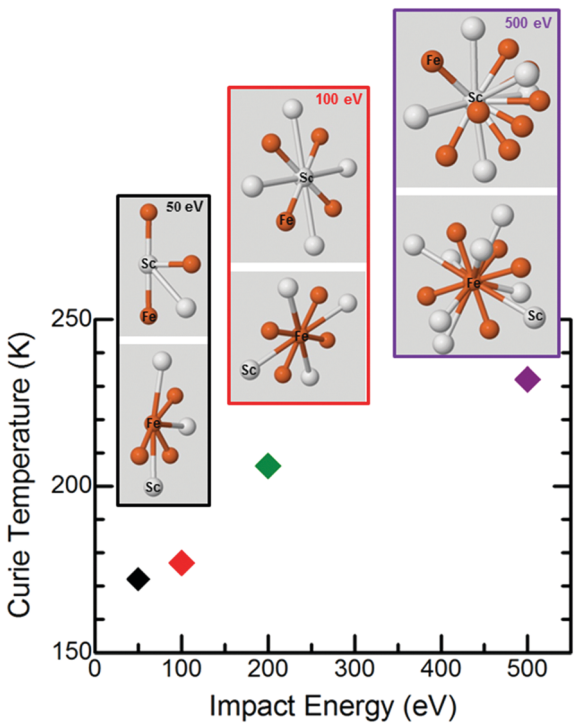

Fig. 6 Evolution of the Curie temperature as a function of the impact energy of the cluster-assembled metallic glasses. The corresponding changes in the local motifs within the amorphous structure (the first neighbors only around Sc and Fe centers are displayed) along with the Curie temperature are presented for 50 (black), 100 (red), 200 (green) and 500 (purple) eV per cluster impact energy. One possible representation of local motifs is presented here.

Fig. 6 shows the observed changes in the Curie temperature, as a function of impact energy, together with one possible

graphical representation of the local motifs based on the results of the EXAFS analysis, in terms of the number of neighboring atoms and their interatomic distances. Additional information on the local motifs such as the spatial arrangements of the atoms cannot be extracted from EXAFS data. The lower Curie temperatures, measured on the samples deposited at the lower impact energies (50, 100, 200 eV per cluster), are in line with the reduced number of spatially correlated nearest neighbors in the respective local motifs. Of course, to fully unravel the physical origins of this correlation, more information is needed on the geometrical configurations of Fe and Sc atoms along with the possible relative orientations of the neighboring local motifs. However, one can notice right away that the Fe–Fe distances between the nearest neighbors are virtually independent of the cluster impact energy. Consequently, when considering the trend in Curie temperature *versus* impact energy, the Fe–Fe distance dependence of the magnetic exchange interactions can be neglected in the first approximation. Thus, the observed increase in the Curie temperature with increasing size of cluster local motifs can be explained within the context of a standard mean-field approximation, strongly suggesting that increasing the number of the Fe nearest neighbors strengthens the magnetic exchange interactions and thus shifts the Curie temperature to the correspondingly higher values.

4. Conclusion

In this study, we establish a clear correlation between the size of the local motifs and the magnetic properties of $Fe_{80}Sc_{20}$ cluster-assembled metallic glass films, deposited at different impact energies, in comparison to a rapidly quenched reference sample. The size of the local motifs increases with increasing impact energy of the clusters; the cluster size for the film sample deposited with the highest impact energy (500 eV per cluster) becomes comparable to that of the rapidly quenched sample. While the fundamental mechanisms responsible for the different atomic structures of the cluster-assembled glasses are not at present fully understood, it is evident that the magnetic properties are closely correlated with the deposition parameters. Therefore, this new deposition method offers an exciting opportunity to tailor the physical properties, especially the magnetic properties, of novel cluster-assembled amorphous materials by fine-tuning the local atomic structure (local motifs) of the cluster-assembled metallic glass samples.

Author contributions

A. F. and H. H. conceived and designed the experimental plan. C. B., A. F. and R. K. took care of the preparation of the samples as well as the acquisition and evaluation of the magnetic property data. A. L., A. Z. and R. S. carried out the XAFS experiments. A. L. and A. Z. conducted the XAFS data analysis. A. L., H. H., R. K., A. Z., C. B. and R. S. discussed the experimental data. A. L. and H. H. wrote the initial draft of the manuscript. Thereafter, all authors contributed to the final preparation of the manuscript.

Conflicts of interest

There are no conflicts of interest to declare.

Acknowledgements

H. H. acknowledges the financial support from the Deutsche Forschungsgemeinschaft under grant HA 1344-38/1 and the large equipment grant provided by the State of Hesse for the Joint Research Laboratory Nanomaterials at Technische Universität Darmstadt. We acknowledge the KIT Light Source for provision of instruments at its beamlines and we would like to thank the Institute for Beam Physics and Technology (IBPT) for the operation of the storage ring, the Karlsruhe Research Accelerator (KARA).

References

1 W. Klement, R. H. Willens and P. Duwez, *Nature*, 1960, **187**, 869.
2 E. Ma and J. Ding, *Mater. Today*, 2016, **19**, 568.
3 Y. Q. Cheng and E. Ma, *Prog. Mater. Sci.*, 2011, **56**, 379.
4 A. Lindsay Greer, *Mater. Today*, 2009, **12**, 14.
5 L. Yang, G. Q. Guo, L. Y. Chen, B. Laqua and J. Z. Jiang, *Intermetallics*, 2014, **44**, 94.
6 H. Wagner, D. Bedorf, S. Küchemann, M. Schwabe, B. Zhang, W. Arnold and K. Samwer, *Nat. Mater.*, 2011, **10**, 439.
7 M. Veligatla, S. Das, W. K. Lee, Y. Hwang, O. Thumthan, Y. Hao and S. Mukherjee, *JOM*, 2016, **68**, 336.
8 J. G. Wang, Y. C. Hu, P. F. Guan, K. K. Song, L. Wang, G. Wang, Y. Pan, B. Sarac and J. Eckert, *Sci. Rep.*, 2017, **s41598-017-07669-9**, 1.
9 D. B. Miracle, *Nat. Mater.*, 2004, **3**, 697.
10 H. W. Sheng, W. K. Luo, F. M. Alamgir, J. M. Bai and E. Ma, *Nature*, 2006, **439**, 419.
11 M. Ghafari, H. Gleiter, T. Feng, K. Ohara and H. Hahn, *J. Mater. Sci. Eng.*, 2016, **5**, 299.
12 A. Hirata, P. Guan, T. Fujita, Y. Hirotsu, A. Inoue, A. R. Yavari, T. Sakurai and M. Chen, *Nat. Mater.*, 2011, **10**, 28.
13 E. Ma, Tuning order in disorder, *Nat. Mater.*, 2015, **14**, 547.
14 A. Kartouzian, J. Antonowicz, T. Lünskens, A. Logogianni, P. Heister, G. Evangelakis and R. Felici, *Mater. Express*, 2014, **4**, 228.
15 A. L. Greer, *Nat. Mater.*, 2015, **14**, 542.
16 A. Fischer, R. Kruk and H. Hahn, *Rev. Sci. Instrum.*, 2015, **86**, 023304.
17 B. Ravel and M. Newville, *J. Synchrotron Radiat.*, 2005, **12**, 537.
18 M. Müller, M. Ghafari, S. H. Banihashemei, B. Stahl and H. Hahn, *Phys. Status Solidi*, 2002, **189**, 1043.